Color Demosaicing Using Variance of Color Differences

King-Hong Chung and Yuk-Hee Chan, *Member, IEEE*

***Abstract*—This paper presents an adaptive demosaicing algorithm. Missing green samples are first estimated based on the variances of the color differences along different edge directions. The missing red and blue components are then estimated based on the interpolated green plane. This algorithm can effectively preserve the details in texture regions and, at the same time, it can significantly reduce the color artifacts. As compared with the latest demosaicing algorithms, the proposed algorithm produces the best average demosaicing performance both objectively and subjectively.**

***Index Terms*—Bayer sampling, color demosaicing, color filter array, digital camera, interpolation.**

I. Introduction

A FULL-COLOR image is usually composed of three color planes and, accordingly, three separate sensors are required for a camera to measure an image. To reduce the cost, many cameras use a single sensor covered with a color filter array (CFA). The most common CFA used nowadays is the Bayer CFA shown in Fig. 1, [1]. In the CFA-based sensor configuration, only one color is measured at each pixel and the missing two color values are estimated. The estimation process is known as color demosaicing [2].

In general, a demosaicing algorithm can be either heuristic or nonheuristic. A heuristic approach does not try to solve a mathematically defined optimization problem while a nonheuristic approach does. Examples of nonheuristic approaches include [3]–[6]. In particular, Gunturk's algorithm (AP) [3] tries to maintain the output image within the "observation" and "detail" constraint sets with the projection-onto-convex-sets (POCS) technique while Muresan's algorithm (DUOR) [4] is an optimal-recovery-based nonlinear interpolation scheme. As for the one in [5] (DSA), it successfully approximates the demosaicing result in color difference domain with a spatially adaptive stopping criterion. Alleyson's algorithm [6] proposed a low-pass and a corresponding high-pass filter for recovering the luminance and chrominance terms via analyzing the characteristics of a CFA image in frequency domain.

Manuscript received August 10, 2005; revised March 10, 2006. This work was supported by the Research Grants Council of the Hong Kong Special Administrative Region, China, under Grant PolyU 5205/04E. The associate editor coordinating the review of this manuscript and approving it for publication was Dr. Luca Lucchese.

The authors are with the Centre for Multimedia Signal Processing, Department of Electronic and Information Engineering, The Hong Kong Polytechnic University, Hong Kong (e-mail: enyhchan@polyu.edu.hk).

Color versions of Figs. 1–9 are available online at http://ieeexplore.ieee.org.
Digital Object Identifier 10.1109/TIP.2006.877521

Most existing demosaicing algorithms are heuristic algorithms. Bilinear interpolation (BI) [7] is the simplest heuristic method, in which the missing samples are interpolated on each color plane independently and high frequency information cannot be preserved well in the output image. With the use of interchannel correlation, algorithms proposed in [8]–[11] attempt to maintain edge detail or limit hue transitions to provide better demosaicing performance. In [12], an effective color interpolation method (ECI) is proposed to get a full color image by interpolating the color differences between green and red/blue plane. The algorithms proposed in [13]–[22] are some of the latest methods. Among them, Wu's algorithm [13] is a primary-consistent soft-decision (PCSD) algorithm which eliminates color artifacts by ensuring the same interpolation direction for each color component of a pixel while Hirakawa's algorithm (AHDDA) [15] uses local homogeneity as an indicator to pick the direction for interpolation. In [16]–[18], [20]–[22], a color-ratio model or a color-difference model cooperating with an edge-sensing mechanism is used to drive the interpolation process along the edges while, in [19], an adaptive demosaicing scheme using bilateral filtering technique is proposed.

To a certain extent, it can be found that a number of heuristic algorithms were developed based on the framework of the adaptive color plane interpolation algorithm (ACPI) proposed in [10]. For example, algorithms in [13] and [15] exploit the same interpolators used in ACPI to generate the green plane. The improved demosaicing performance of these advanced heuristic algorithms is generally achieved by that they can interpolate the missing samples along a correct direction. In this paper, based on the framework of ACPI, a new heuristic demosaicing algorithm is proposed. This algorithm uses the variance of pixel color differences to determine the interpolation direction for interpolating the missing green samples. Simulation results show that the proposed algorithm is superior to the latest demosaicing algorithms in terms of both subjective and objective criteria. In particular, it can outstandingly preserve the texture details in an image.

The paper is organized as follows. In Section II, we revisit the ACPI algorithm [10]. An analysis is made and our motivation to develop the proposed algorithm is presented. Section III presents the details of our demosaicing algorithm, and Section IV presents some simulation results for comparison study. Finally, a conclusion is given in Section V.

II. Observations on the Adaptive Interpolation Algorithm

In ACPI [10], the green plane is handled first and the other color planes are handled based on the estimation result of the green plane. When the green plane is processed, for each

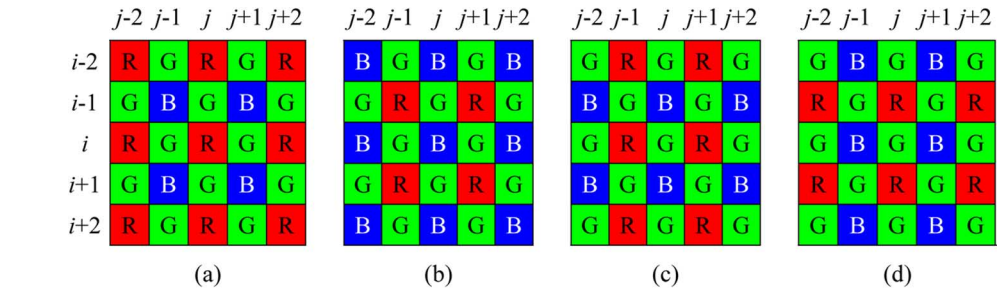

Fig. 1. Four 5 × 5 regions of Bayer CFA pattern having their centers at (a) red, (b) blue, and (c)–(d) green CFA samples.

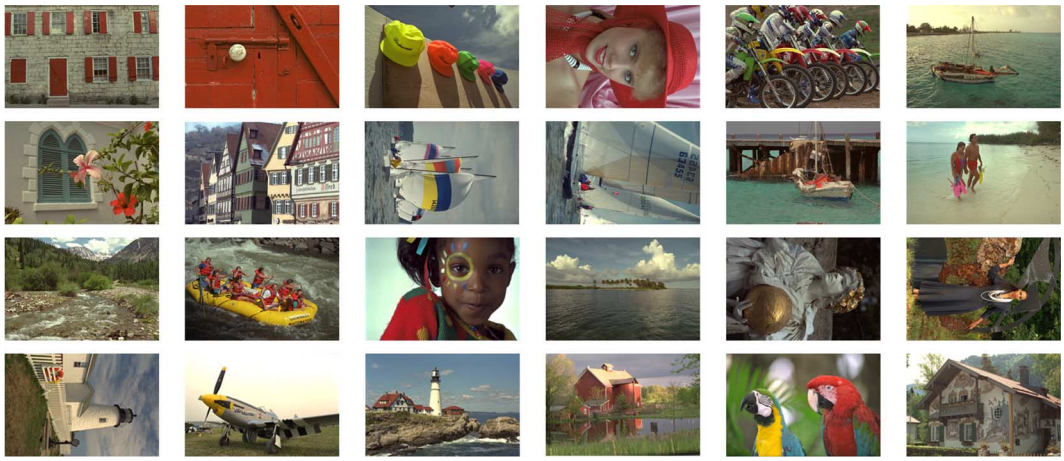

Fig. 2. Set of testing images (Refers as image 1 to image 24, from top-to-bottom and left-to-right).

missing green component in the CFA, the algorithm performs a gradient test and then carries out an interpolation along the direction of a smaller gradient to determine the missing green component. A pixel without green component in the Bayer CFA may have a neighborhood as shown in either Fig. 1(a) or Fig. 1(b). Without losing the generality, here, we consider the former case only. In this case, the horizontal gradient $\Delta H_{i,j}$ and the vertical gradient $\Delta V_{i,j}$ at position (i, j) are estimated first to determine the interpolation direction as follows:

$$\Delta H_{i,j} = |G_{i,j-1} - G_{i,j+1}| + |2R_{i,j} - R_{i,j-2} - R_{i,j+2}| \quad (1)$$

$$\Delta V_{i,j} = |G_{i-1,j} - G_{i+1,j}| + |2R_{i,j} - R_{i-2,j} - R_{i+2,j}| \quad (2)$$

where $R_{m,n}$ and $G_{m,n}$ denote the known red and green CFA components at position (m, n). Based on the values of $\Delta H_{i,j}$ and $\Delta V_{i,j}$, the missing green component $g_{i,j}$ in Fig. 1(a) is interpolated as follows:

$$g_{i,j} = \frac{(G_{i,j-1} + G_{i,j+1})}{2} + \frac{(2R_{i,j} - R_{i,j-2} - R_{i,j+2})}{4} \quad \text{if } \Delta H_{i,j} < \Delta V_{i,j} \quad (3)$$

$$g_{i,j} = \frac{(G_{i-1,j} + G_{i+1,j})}{2} + \frac{(2R_{i,j} - R_{i-2,j} - R_{i+2,j})}{4} \quad \text{if } \Delta H_{i,j} > \Delta V_{i,j} \quad (4)$$

$$g_{i,j} = \frac{(G_{i-1,j} + G_{i+1,j} + G_{i,j-1} + G_{i,j+1})}{4} + \frac{(4R_{i,j} - R_{i-2,j} - R_{i+2,j} - R_{i,j-2} - R_{i,j+2})}{8} \quad \text{if } \Delta H_{i,j} = \Delta V_{i,j}. \quad (5)$$

In fact, it was shown in [15] that (3) and (4) were the approximated optimal CFA interpolators in horizontal and vertical directions and (5) was good enough for interpolating diagonal image features.

Since the red and the blue color planes are determined based on the estimation result of the green plane and the missing green components are in turns determined by the result of the gradient test, the demosaicing result highly relies on the success of the gradient test. A study was performed here to evaluate how significant the gradient test is to the performance of the algorithm.

In a simulation of our study, twenty-four 24-bit (of bit ratio R : G : B = 8 : 8 : 8) digital color images of size 512 × 768 pixels each as shown in Fig. 2 were sampled according to Bayer CFA to form a set of testing images. These images are part of the Kodak color image database and include various scenes. The testing images were reconstructed with ACPI [10] and the ideal ACPI. The ideal ACPI is basically ACPI except that, in determining a missing green component, it computes all $g_{i,j}$ estimates with (3-5) and picks the one closest to the real value of the missing component without performing any gradient test. Note that, in this simulation, all original images are known, and, hence, the real value of a missing green component of the testing images can be used to implement the ideal ACPI. In practice, the original images are not known, and, hence, the performance of the ideal ACPI is practically unachievable. The ideal ACPI is only used as a reference in our study.

We measured the peak signal-to-noise ratios (PSNRs) of the interpolated green planes of both ACPI [10] and the ideal APCI with respect to the original green plane. We found that the average PSNR achieved by the ideal ACPI was 43.83 dB while that achieved by ACPI was only 38.18 dB. This implies that

TABLE I
CPSNR PERFORMANCE (IN DECIBELS) OF VARIOUS ALGORITHMS

Image	Non-heuristic algorithms			Heuristic algorithms									
	AP [3]	DUOR [4,27]	DSA [5]	BI [7]	ACPI [10]	ECI [12]	PCSD [13]	DAFD [16]	EECI [14]	AHDDA [15]	Ours w/o refinement	Ours with refinement	Ideal ACPI
1	37.70	34.66	38.32	26.21	33.59	33.81	36.40	35.92	37.99	35.16	35.97	38.53	38.83
2	39.57	39.22	39.95	33.08	39.00	38.88	39.67	39.70	40.49	39.19	39.68	40.43	42.32
3	41.45	41.18	41.18	34.45	40.50	40.87	41.77	41.00	42.64	41.59	41.72	42.54	43.69
4	40.03	38.56	39.55	33.46	38.50	39.43	39.53	39.64	40.51	38.94	39.60	40.50	41.51
5	37.46	35.25	36.48	26.51	34.79	35.29	37.17	36.15	38.04	35.74	36.15	37.89	38.81
6	38.50	37.87	39.08	27.66	34.79	34.95	38.86	36.94	38.10	37.57	38.01	40.03	40.64
7	41.77	41.39	41.50	33.38	40.84	40.54	41.48	41.03	42.73	40.92	41.02	42.15	43.69
8	35.08	31.04	35.87	23.39	32.04	30.52	34.48	33.34	35.20	33.77	34.25	36.41	36.93
9	41.72	41.27	41.94	32.16	40.15	39.55	41.99	40.73	42.58	41.09	41.63	43.04	44.01
10	42.02	40.39	41.80	32.38	39.84	40.30	41.75	41.13	42.52	40.71	41.20	42.51	43.48
11	39.14	37.42	38.92	28.96	35.97	36.24	38.57	38.09	39.46	37.53	37.99	39.86	40.94
12	42.51	42.30	42.37	33.27	40.53	40.02	42.61	41.13	42.63	41.75	42.09	43.45	44.22
13	34.30	31.08	34.91	23.79	29.65	31.33	32.85	33.64	34.38	31.52	32.32	34.90	35.15
14	35.60	35.58	34.52	29.05	35.43	35.43	35.44	35.52	37.13	35.49	36.08	36.88	38.96
15	39.35	37.77	38.97	33.04	37.61	38.94	38.93	39.09	39.49	38.03	38.95	39.78	41.15
16	41.76	41.82	41.60	31.13	38.33	37.91	42.73	40.14	41.16	41.40	41.64	43.64	44.02
17	41.11	39.06	40.97	31.80	38.28	39.26	40.49	40.44	41.36	39.42	39.84	41.21	42.50
18	37.45	35.28	37.27	28.30	34.38	35.79	36.35	37.01	37.73	35.31	35.81	37.49	38.64
19	39.46	38.06	39.96	27.84	37.27	35.29	39.54	37.39	40.13	38.48	39.28	41.00	42.00
20	40.66	39.05	40.51	31.51	38.48	38.70	40.05	40.09	41.33	39.27	39.67	41.07	42.03
21	38.66	36.22	38.93	28.38	35.13	35.72	37.36	37.62	38.96	36.55	37.12	39.12	39.88
22	37.55	36.49	37.67	30.14	36.16	36.45	37.06	37.08	38.28	36.51	37.08	37.97	39.83
23	41.88	41.34	41.79	34.83	41.70	41.68	42.15	41.62	42.91	41.85	42.22	42.89	44.46
24	34.78	32.49	34.82	26.83	32.15	33.76	34.58	34.28	34.82	33.64	34.12	35.04	36.82
Avg.	**39.15**	**37.70**	**39.12**	**30.06**	**36.88**	**37.11**	**38.83**	**38.28**	**39.61**	**37.98**	**38.48**	**39.93**	**41.02**

there is a great room for improving the performance of ACPI. Based on this simulation result, we have two observations. First, the interpolators used in [10] can be very effective if there is an "effective" gradient test to provide some reliable guidance for the interpolation. Second, the current gradient test used in [10] is not good enough.

After having the "ideal" green plane with the ideal ACPI, we proceeded to interpolate the red and the blue planes with it to produce a full color image with the same procedures as originally proposed in ACPI. The quality of the output was measured in terms of color-peak signal-to-noise ratio (CPSNR) which is defined in (24). As expected, it achieves extremely high score, and, subjectively, it is hard to distinguish the recovered image from the original full color image. Table I shows the performance of various algorithms for comparison. As shown in Table I, the ideal ACPI provides a very outstanding performance as compared with any other evaluated demosaicing algorithms. This shows that the approach used in [10] to derive the other color planes with a "good" green plane is actually very effective. As a good green plane relies on a good gradient test, the key of success is again the effectiveness of the gradient test or, to be more precise, the test for determining the interpolation direction. This finding motivates the need to find an effective and efficient gradient test to improve the performance of ACPI.

When we probed into the gradient test used in [10], we found that the test encountered problems when dealing with pixels in texture regions. Fig. 3 shows an example where the test does not work properly. A 5×5 block located in a texture region is extracted for inspection as shown in Fig. 3(a). Fig.3(b) and (c) shows, respectively, the pixel values of the vertical and the horizontal lines across the block center. Suppose the black dots in the plots are the CFA samples while the others are the samples needed to be estimated. Consider that we are going to estimate the green component of the block center. As the black dash lines in vertical direction are flatter than that in horizontal direction, the test provides a misleading result. The algorithm interpolates vertically to determine the missing green component although it should interpolate horizontally. That is the reason why details cannot be preserved in a texture region with ACPI.

In summary, the ACPI algorithm can perform outstandingly if all the missing green samples are interpolated in appropriate directions. Thus, the determination of the interpolation direction for the missing green samples, in turn, becomes the ghost of the demosaicing method.

III. PROPOSED ALGORITHM

Based on the observations presented in Section II, the proposed algorithm put its focus on how to effectively determine the interpolation direction for estimating a missing green component in edge regions and texture regions. In particular, variance of color differences is used in the proposed algorithm as a

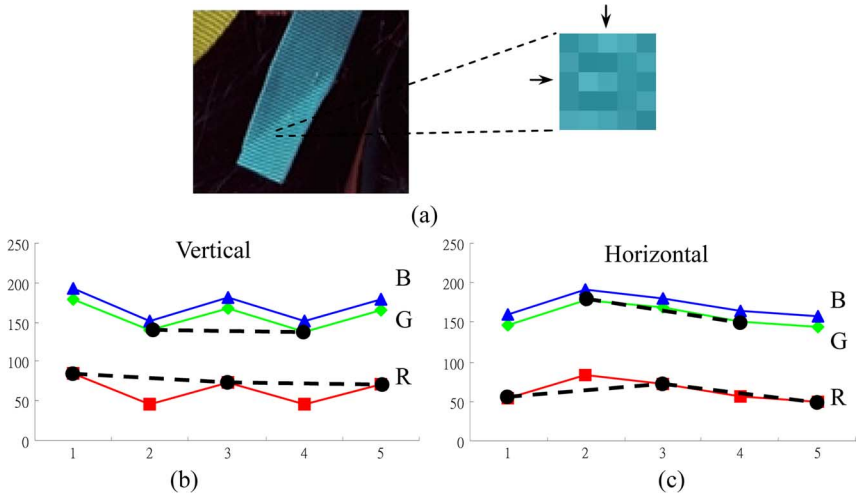

Fig. 3. Example where a simple gradient test does not work: (a) a 5 × 5 block in texture region, (b) pixel values along the vertical line across the block center, and (c) pixel values along the horizontal line across the block center.

supplementary criterion to determine the interpolation direction for the green components.

For the sake of reference, hereafter, a pixel at location (i,j) in the CFA is represented by either $(R_{i,j}, g_{i,j}, b_{i,j})$, $(r_{i,j}, G_{i,j}, b_{i,j})$ or $(r_{i,j}, g_{i,j}, B_{i,j})$, where $R_{i,j}, G_{i,j}$, and $B_{i,j}$ denote the known red, green, and blue components, and $r_{i,j}, g_{i,j}$ and $b_{i,j}$ denote the unknown components in the CFA. The estimates of $r_{i,j}, g_{i,j}$, and $b_{i,j}$ are denoted as $\hat{R}_{i,j}, \hat{G}_{i,j}$, and $\hat{B}_{i,j}$. To get $\hat{R}_{i,j}, \hat{G}_{i,j}$, and $\hat{B}_{i,j}$, preliminary estimates of $r_{i,j}, g_{i,j}$, and $b_{i,j}$ may be required in the proposed demosaicing algorithm. These intermediate estimates are denoted as $\hat{r}_{i,j}, \hat{g}_{i,j}$, and $\hat{b}_{i,j}$.

A. Interpolating Missing Green Components

In the proposed algorithm, the missing green components are first interpolated in a raster scan manner. As far as a missing green component in the Bayer CFA is concerned, its neighborhood must be in a form as shown in either Fig. 1(a) or Fig. 1(b). Without losing the generality, let us consider the case shown in Fig. 1(a) only. For the other case, the same treatment used in this case can be done to estimate the missing green component by exchanging the roles of the red components and the blue components.

In Fig. 1(a), the center pixel $p_{i,j}$ is represented by $(\mathrm{R}_{i,j}, \mathrm{g}_{i,j}, \mathrm{b}_{i,j})$, where $g_{i,j}$ is the missing green component needed to be estimated. The proposed algorithm computes the two following parameters instead of $\Delta H_{i,j}$ and $\Delta V_{i,j}$ as in the ACPI algorithm:

$$\begin{aligned} L^H = \sum_{n=\pm 2} \Bigg[& \sum_{m=0,\pm 2} |R_{i+m,j+n} - R_{i+m,j}| \\ & + \sum_{m=\pm 1} |G_{i+m,j+n} - G_{i+m,j}| \Bigg] \\ & + \sum_{n=\pm 1} \Bigg[\sum_{m=0,\pm 2} |G_{i+m,j+n} - R_{i+m,j}| \\ & + \sum_{m=\pm 1} |B_{i+m,j+n} - G_{i+m,j}| \Bigg] \end{aligned} \tag{6}$$

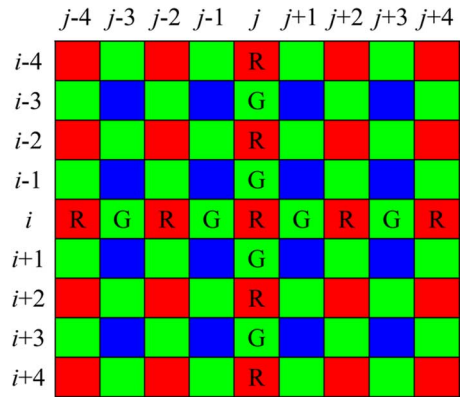

Fig. 4. A 9 × 9 window of Bayer CFA pattern.

$$\begin{aligned} L^V = \sum_{m=\pm 2} \Bigg[& \sum_{n=0,\pm 2} |R_{i+m,j+n} - R_{i,j+n}| \\ & + \sum_{n=\pm 1} |G_{i+m,j+n} - G_{i,j+n}| \Bigg] \\ & + \sum_{m=\pm 1} \Bigg[\sum_{n=0,\pm 2} |G_{i+m,j+n} - R_{i,j+n}| \\ & + \sum_{n=\pm 1} |B_{i+m,j+n} - G_{i,j+n}| \Bigg]. \end{aligned} \tag{7}$$

These two parameters are used to estimate whether there is sharp horizontal or vertical gradient change in the 5 × 5 testing window (with $p_{i,j}$ as the window center). A large value implies that there exists a sharp gradient change along a particular direction. The ratio of the two parameters is then computed to determine the dominant edge direction

$$e = \max\left(\frac{L^V}{L^H}, \frac{L^H}{L^V}\right). \tag{8}$$

A block is defined to be a sharp edge block if $e > T$, where T is a predefined threshold value to be discussed in more details in

Section IV. If a block is a sharp edge block, the missing green component of the block center is interpolated as follows:

$$g_{i,j} = \frac{(G_{i,j-1} + G_{i,j+1})}{2} + \frac{(2R_{i,j} - R_{i,j-2} - R_{i,j+2})}{4} \quad \text{if } L^{\mathrm{H}} < L^{V} \tag{9}$$

$$g_{i,j} = \frac{(G_{i-1,j} + G_{i+1,j})}{2} + \frac{(2R_{i,j} - R_{i-2,j} - R_{i+2,j})}{4} \quad \text{if } L^{\mathrm{H}} > L^{V}. \tag{10}$$

The block classifier based on (6)–(8) and threshold T is used to detect sharp edge blocks and determine the corresponding edge direction for interpolation. In (6) and (7), both inter-band and intraband color information is used to evaluate parameters L^{V} and L^{H}. The first summation terms of (6) and (7) contribute the intraband information, which involves the difference between a pixel and its second next pixel. Obviously, the resolution that it supports cannot detect a sharp line of width 1 pixel. The supplementary intraband color information contributed in the second summation terms of (6) and (7) is used to improve the resolution of the edge detector.

A block which is not classified to be an edge block is considered to be in a flat region or a pattern region. It was found that, in a local region of a natural image, the color differences of pixels are more or less the same [23]. Accordingly, the variance of color differences can be used as supplementary information to determine the interpolation direction for the green components.

In the proposed algorithm, we extend the 5×5 block of interest into a 9×9 block by including more neighbors as shown in Fig. 4 and evaluate the color differences of the pixels along the axis within the 9×9 window. Let ${}_{H}\sigma^{2}_{i,j}$ and ${}_{V}\sigma^{2}_{i,j}$ be, respectively, the variances of the color differences of the pixels along the horizontal axis and the vertical axis of the 9×9 block. In particular, they are defined as

$${}_{H}\sigma^{2}_{i,j} = \frac{1}{9}\sum_{n\in\Psi}\left(d_{i,j+n} - \frac{1}{9}\sum_{k\in\Psi} d_{i,j+k}\right)^{2} \tag{11}$$

and

$${}_{V}\sigma^{2}_{i,j} = \frac{1}{9}\sum_{n\in\Psi}\left(d_{i+n,j} - \frac{1}{9}\sum_{k\in\Psi} d_{i+k,j}\right)^{2} \tag{12}$$

where $d_{p,q}$ is the color difference of pixel (p,q) and $\Psi = \{0, \pm1, \pm2, \pm3, \pm4\}$ is a set of indexes which helps to identify a pixel in the 9×9 support region. The values of $d_{i,j+n}$ and $d_{i+n,j}$ for $n \in \Psi$ should be precomputed and they are determined sequentially as follows:

$$d_{i,j+n} = \begin{cases} R_{i,j+n} - \hat{G}_{i,j+n} & \text{if } n = -2, -4 \\ R_{i,j+n} - \hat{g}_{i,j+n} & \text{if } n = 0, 2, 4 \end{cases} \tag{13}$$

$$d_{i+n,j} = \begin{cases} R_{i+n,j} - \hat{G}_{i+n,j} & \text{if } n = -2, -4 \\ R_{i+n,j} - \hat{g}_{i+n,j} & \text{if } n = 0, 2, 4 \end{cases} \tag{14}$$

$$d_{i,j+n} = (d_{i,j+n-1} + d_{i,j+n+1})/2 \quad \text{for } n = \pm1, \pm3 \tag{15}$$

and

$$d_{i+n,j} = (d_{i+n-1,j} + d_{i+n+1,j})/2 \quad \text{for } n = \pm1, \pm3. \tag{16}$$

Here, bilinear interpolation is used with the concern about the realization complexity to estimate $d_{i,j+n}$ and $d_{i+n,j}$ for $n = \pm1, \pm3$. In fact, there was no obvious improvement in the simulation results when other interpolation schemes such as cubic interpolation were used.

To provide some more information about (13) and (14), we note that the missing green components are estimated in a raster scan fashion, and, hence, the final estimates of the green components in position $\Omega_{i,j} = \{(i, j+n), (i+n, j) | n = -2, -4\}$ are already computed. As for the missing green components of the pixels in position $\{(i, j+n), (i+n, j) | n = 0, 2, 4\}$, their preliminary estimates $\hat{g}_{i,j+n}$ and $\hat{g}_{i+n,j}$ have to be evaluated. Specifically, $\hat{g}_{i,j+n}$ is determined with (3) while $\hat{g}_{i+n,j}$ is determined with (4) unconditionally. Note the $d_{i,j}$ involved in (11) uses the $\hat{g}_{i,j}$ determined with (3) while the $d_{i,j}$ involved in (12) uses the $\hat{g}_{i,j}$ determined with (4).

The variance of the color differences of the diagonal pixels in the 9×9 window, say ${}_{B}\sigma^{2}_{i,j}$, are determined by

$${}_{B}\sigma^{2}_{i,j} = \frac{1}{2}\left(\frac{1}{9}\sum_{n\in\Psi}\left(d_{i+n,j} - \frac{1}{9}\sum_{k\in\Psi} d_{i+k,j}\right)^{2} + \frac{1}{9}\sum_{n\in\Psi}\left(d_{i,j+n} - \frac{1}{9}\sum_{k\in\Psi} d_{i,j+k}\right)^{2}\right). \tag{17}$$

The same set of (13)–(16) are used to get the color difference $d_{p,q}$ required in the evaluation of ${}_{B}\sigma^{2}_{i,j}$. However, the preliminary estimates $\hat{g}_{i,j+n}$ and $\hat{g}_{i+n,j}$ involved in these equations are determined with (5) instead of (3) and (4).

Finally, the interpolation direction for estimating the missing green component at $p_{i,j} = (\mathrm{R}_{i,j}, \mathrm{g}_{i,j}, \mathrm{b}_{i,j})$ can be determined based on ${}_{H}\sigma^{2}_{i,j}$, ${}_{V}\sigma^{2}_{i,j}$, and ${}_{B}\sigma^{2}_{i,j}$. It is the direction providing the minimum variance of color difference. The missing green $g_{i,j}$ can then be estimated with either formulation (3), (4), or (5) without concerning $\Delta H_{i,j}$ and $\Delta V_{i,j}$, as shown in (18), at the bottom of the page.

Once the missing green component is interpolated, the same process is performed for estimating the next missing green component in a raster scan manner. For estimating the missing green component in the case shown in Fig. 1(b), one can replace the red samples by the corresponding blue samples and follow the

$$\hat{G}_{i,j} = \begin{cases} \text{unconditional evaluation result of (3)} & \text{if } {}_{H}\sigma^{2}_{i,j} = \min({}_{H}\sigma^{2}_{i,j}, {}_{V}\sigma^{2}_{i,j}, {}_{B}\sigma^{2}_{i,j}) \\ \text{unconditional evaluation result of (4)} & \text{if } {}_{V}\sigma^{2}_{i,j} = \min({}_{H}\sigma^{2}_{i,j}, {}_{V}\sigma^{2}_{i,j}, {}_{B}\sigma^{2}_{i,j}) \\ \text{unconditional evaluation result of (5)} & \text{if } {}_{B}\sigma^{2}_{i,j} = \min({}_{H}\sigma^{2}_{i,j}, {}_{V}\sigma^{2}_{i,j}, {}_{B}\sigma^{2}_{i,j}) \end{cases} \tag{18}$$

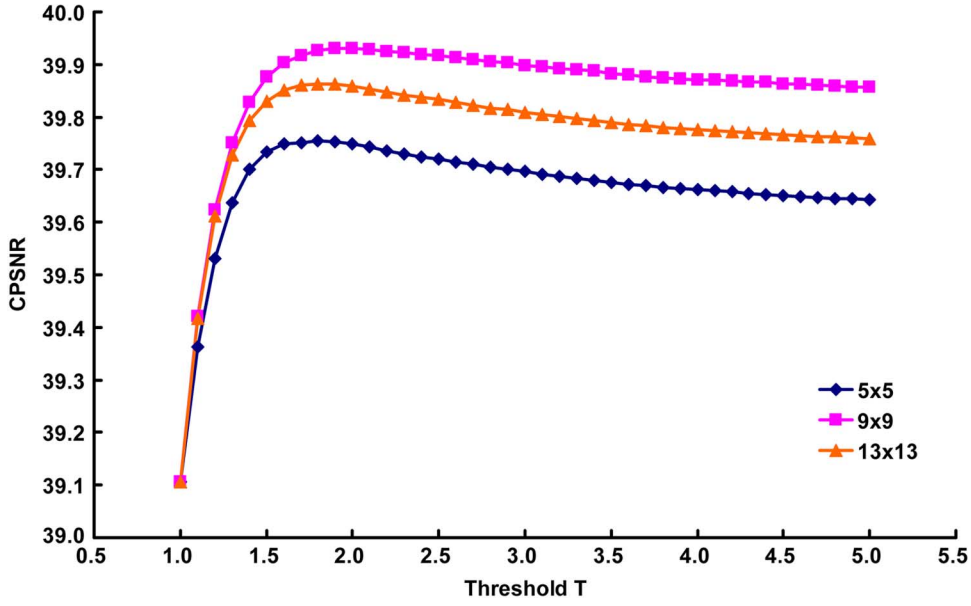

(a)

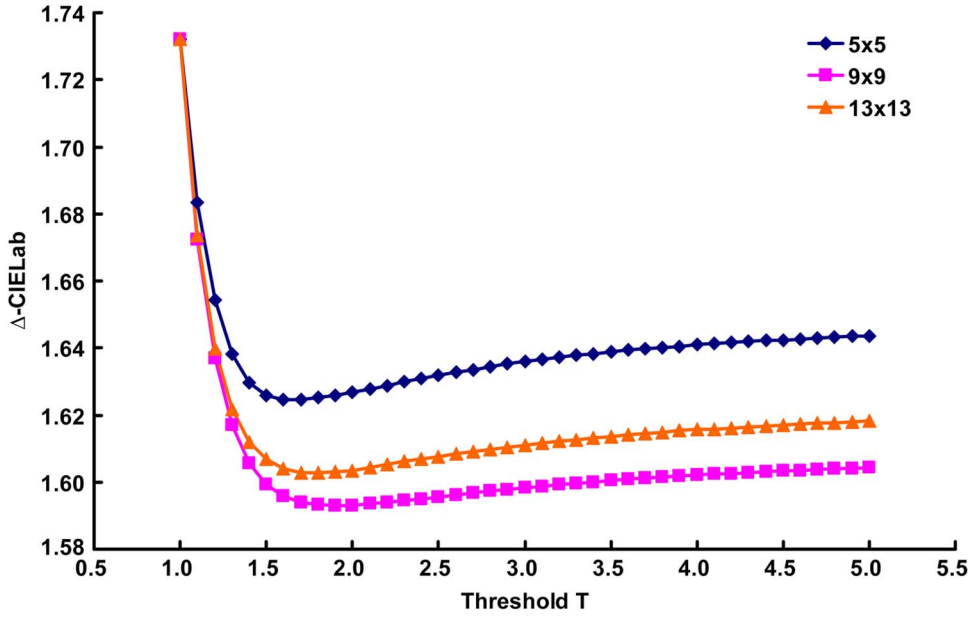

(b)

Fig. 5. Performance of the proposed algorithm at different settings of threshold T and window size. (a) CPSNR. (b) CIELab color difference.

procedures above to determine its interpolation direction and its interpolated value.

The complexity of the realization of (18) and its preparation work (11)–(17) is large. When $e > T$, a sharp edge block is clearly identified. In that case, using (9) and (10) to interpolate missing components can save a lot of effort and, at the same time, provide a good demosacing result.

B. Interpolating Missing Red and Blue Components at Green CFA Sampling Positions

After interpolating all missing green components of the image, the missing red and blue components at green CFA sampling positions are estimated. Fig. 1(c) and (d) shows the two possible cases where a green CFA sample is located at the center of a 5×5 block. For the case shown in Fig. 1(c), the missing components of the center are obtained by

$$\hat{R}_{i,j} = G_{i,j} + \frac{R_{i,j-1} - \hat{G}_{i,j-1} + R_{i,j+1} - \hat{G}_{i,j+1}}{2} \quad (19)$$

$$\hat{B}_{i,j} = G_{i,j} + \frac{B_{i-1,j} - \hat{G}_{i-1,j} + B_{i+1,j} - \hat{G}_{i+1,j}}{2}. \quad (20)$$

As for the case shown in Fig. 1(d), the missing components of the center are obtained by

$$\hat{R}_{i,j} = G_{i,j} + \frac{R_{i-1,j} - \hat{G}_{i-1,j} + R_{i+1,j} - \hat{G}_{i+1,j}}{2} \quad (21)$$

$$\hat{B}_{i,j} = G_{i,j} + \frac{B_{i,j-1} - \hat{G}_{i,j-1} + B_{i,j+1} - \hat{G}_{i,j+1}}{2}. \quad (22)$$

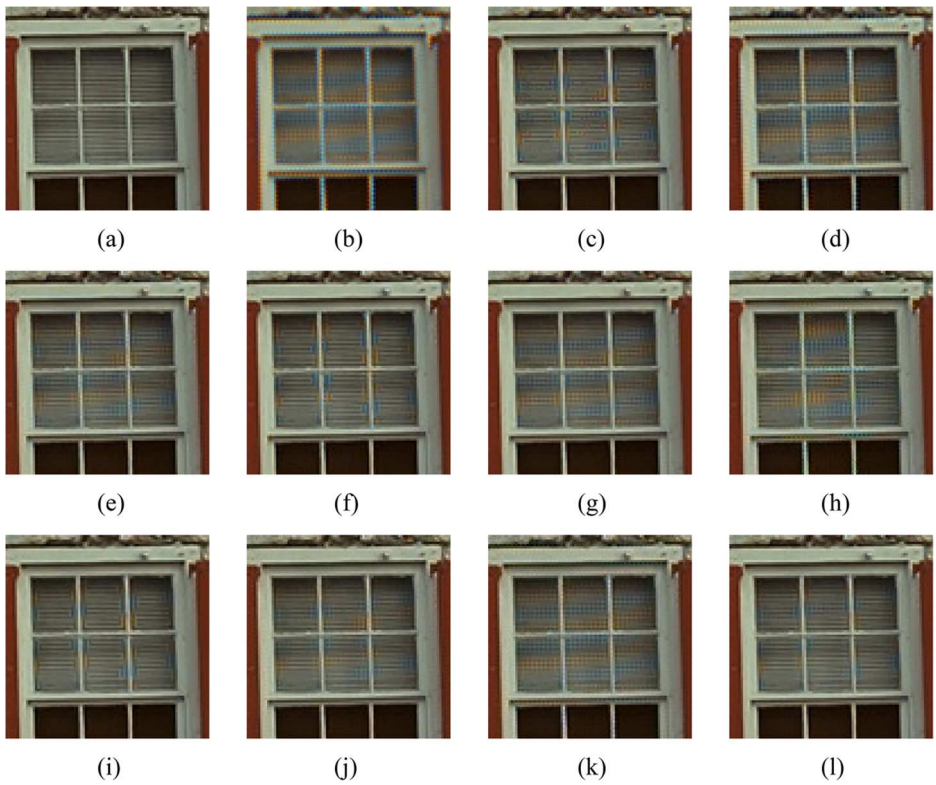

Fig. 6. Part of the demosaicing results of Image 1: (a) The original, (b) BI, (c) ACPI, (d) ECI, (e) AP, (f) PCSD, (g) EECI, (h) DUOR, (i) AHDDA, (j) DSA, (k) DAFD, and (l) the proposed algorithm.

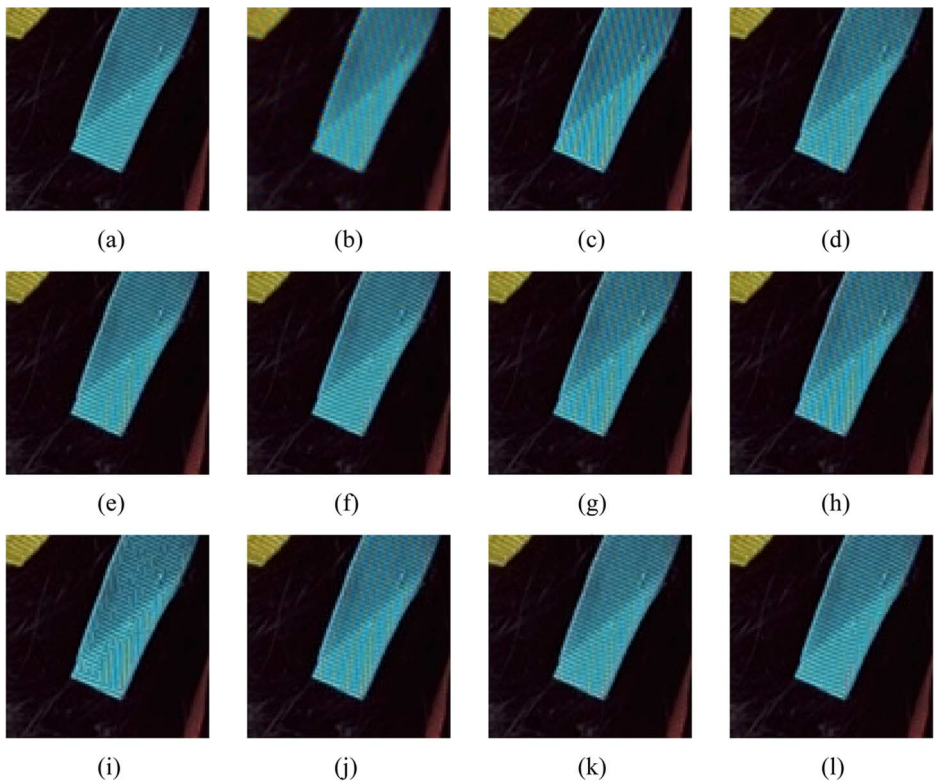

Fig. 7. Part of the demosaicing results of Image 15: (a) The original, (b) BI, (c) ACPI, (d) ECI, (e) AP, (f) PCSD, (g) EECI, (h) DUOR, (i) AHDDA, (j) DSA (k) DAFD, and (l) the proposed algorithm.

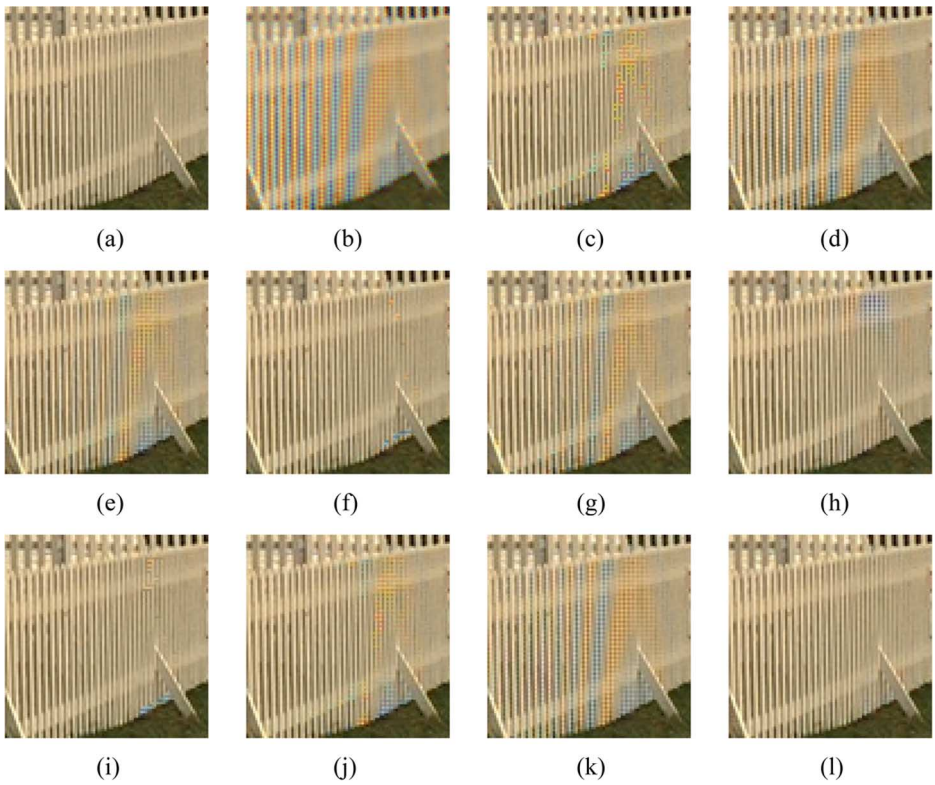

Fig. 8. Part of the demosaicing results of Image 19: (a) The original, (b) BI, (c) ACPI, (d) ECI, (e) AP, (f) PCSD, (g) EECI, (h) DUOR, (i) AHDDA, (j) DSA, and (k) the proposed algorithm.

C. Interpolating Missing Blue (Red) Components at Red (Blue) Sampling Positions

Finally, the missing blue (red) components at the red (blue) sampling positions are interpolated. Fig. 1(a) and (b) shows the two possible cases where the pixel of interest lies in the center of a 5×5 window. For the case in Fig. 1(a), the center missing blue sample, $b_{i,j}$, is interpolated by

$$\hat{B}_{i,j} = \hat{G}_{i,j} + \frac{1}{4} \sum_{m=\pm 1} \sum_{n=\pm 1} (B_{i+m,j+n} - \hat{G}_{i+m,j+n}). \quad (23)$$

As for the case in Fig. 1(b), the center missing red sample, $r_{i,j}$, can also be obtained with (23) by replacing the blue estimates with the corresponding red estimates in (23). At last, the final full color image can be obtained.

D. Refinement

Refinement schemes are usually exploited to further improve the performance of the interpolation in various demosaicing algorithms [11], [13]–[16], [20]–[22]. In fact, there are even some postprocessing methods proposed as stand-alone solutions to improve the quality of a demosaicing result [24], [25]. In the proposed algorithm, we use the refinement scheme suggested in the enhanced ECI algorithm [14] as we found that it matched the proposed algorithm to provide the best demosaicing result after evaluating some other refinement schemes with the proposed algorithm. This refinement scheme processes the interpolated green samples $\hat{G}_{i,j}$ first to reinforce the interpolation performance and, based on the refined green plane, it performs a refinement on the interpolated red and blue samples. One can see [14] for more details on the refinement scheme.

IV. Simulation Results

Simulation was carried out to evaluate the performance of the proposed algorithm. The 24 digital color images shown in Fig. 2 were used to generate a set of testing images as mentioned in Section II. The CPSNR was used as a measure to quantify the performance of the demosaicing methods. In particular, it is defined as

$$\mathrm{CPSNR} = 10 \log_{10} \left(\frac{255^2}{\mathrm{CMSE}} \right) \quad (24)$$

where

$$\mathrm{CMSE} = (1/3\mathrm{HW}) \sum_{i=r,g,b} \sum_{y=1}^{H} \sum_{x=1}^{W} (I_o(x,y,i) - I_r(x,y,i))^2.$$

I_o and I_r represent, respectively, the original and the reconstructed images of size $H \times W$ each.

In the proposed algorithm, a pixel is interpolated according to the nature of its local region. The 5×5 region centered at the pixel is first classified to be either a sharp edge block or not with threshold T. A nonedge block is then extended from 5×5 to 9×9 to compute ${}_H\sigma^2_{i,j}$,${}_V\sigma^2_{i,j}$, and ${}_B\sigma^2_{i,j}$ for further classification. An empirical study was carried out to select an appropriate threshold value of T and check if 9×9 is an appropriate size of the extended local region for estimating ${}_H\sigma^2_{i,j}$,${}_V\sigma^2_{i,j}$, and ${}_B\sigma^2_{i,j}$

TABLE II
PERFORMANCE OF VARIOUS ALGORITHMS IN TERMS OF CIELAB COLOR DIFFERENCE

Image	Non-heuristic algorithms			Heuristic algorithms									
	AP [3]	DUOR [4,27]	DSA [5]	BI [7]	ACPI [10]	ECI [12]	PCSD [13]	DAFD [16]	EECI [14]	AHDDA [15]	Ours w/o refinement	Ours with refinement	Ideal ACPI
1	2.1951	2.7929	2.0857	6.9234	3.1959	3.1093	2.3132	2.6083	2.0318	2.1596	2.4962	1.9593	1.8321
2	1.6534	1.6961	1.5998	2.7510	1.6841	1.7286	1.5883	1.6261	1.4975	1.6005	1.5849	1.4962	1.2211
3	1.0939	1.1618	1.1348	2.1091	1.2497	1.1894	1.0695	1.1579	0.9997	1.0488	1.1061	1.0121	0.8753
4	1.5918	1.8026	1.6831	2.8698	1.8506	1.6775	1.6654	1.6495	1.5132	1.6382	1.6509	1.5194	1.3317
5	2.1541	2.6927	2.3832	6.1880	2.7734	2.6353	2.1215	2.5646	1.9789	2.1745	2.3946	2.0273	1.8082
6	1.7629	1.7609	1.6761	5.1483	2.3906	2.4066	1.5949	2.0347	1.7369	1.5894	1.8065	1.5040	1.3980
7	1.2664	1.2981	1.3179	2.4452	1.3490	1.4015	1.2593	1.3798	1.1341	1.2712	1.3087	1.1935	1.0149
8	2.6797	3.5016	2.4892	8.5984	3.3803	4.0250	2.5900	3.1557	2.4474	2.4800	2.7809	2.2861	2.1051
9	1.2942	1.3418	1.2845	2.7976	1.4870	1.4849	1.2476	1.4124	1.2079	1.2655	1.2992	1.1749	1.0313
10	1.2686	1.4081	1.2808	2.7089	1.4832	1.4068	1.2614	1.3852	1.1941	1.2953	1.3233	1.2020	1.0523
11	1.6774	1.8338	1.6781	4.3695	2.1548	2.1592	1.6439	1.8283	1.5632	1.6188	1.7914	1.5230	1.3303
12	1.1438	1.1639	1.1586	2.4835	1.3577	1.3627	1.1153	1.2690	1.0998	1.1162	1.1827	1.0528	0.9476
13	3.0422	3.9801	2.8736	8.9385	4.8565	4.0087	3.4116	3.2657	2.9006	3.1335	3.6886	2.8559	2.6077
14	2.1081	2.2134	2.2754	4.6786	2.4424	2.3816	2.1065	2.2009	1.8860	2.0246	2.1468	1.9011	1.5915
15	1.4896	1.7072	1.5575	2.6978	1.7676	1.5655	1.5587	1.5607	1.4296	1.5615	1.5689	1.4306	1.2258
16	1.3657	1.2987	1.3491	3.6319	1.7686	1.8403	1.2310	1.5347	1.3694	1.2278	1.3746	1.1715	1.0930
17	1.3120	1.4781	1.3240	2.9295	1.6689	1.5384	1.3693	1.3853	1.2719	1.3612	1.4654	1.2938	1.1332
18	2.1519	2.5223	2.2502	4.8417	2.7406	2.3925	2.3095	2.2306	2.0536	2.2758	2.4023	2.1152	1.7496
19	1.7019	1.8779	1.6166	4.6739	2.0545	2.2889	1.6574	1.8830	1.5670	1.6290	1.7271	1.5029	1.3173
20	1.3160	1.4640	1.3288	2.6634	1.5736	1.5181	1.3626	1.3894	1.2311	1.3358	1.4135	1.2688	1.1254
21	1.7943	2.0671	1.7534	4.5763	2.4541	2.2627	1.9105	1.9516	1.6960	1.8171	2.0363	1.7029	1.5235
22	2.0209	2.2715	2.0630	3.9068	2.3258	2.1663	2.1026	2.0931	1.8905	2.1140	2.1364	1.9576	1.5651
23	1.1955	1.2727	1.2345	1.9242	1.2594	1.2185	1.2077	1.2206	1.1272	1.1917	1.2076	1.1429	0.9530
24	2.0345	2.4735	2.0804	4.8848	2.5768	2.3576	2.0625	2.2244	1.9014	2.0783	2.2044	1.9392	1.6510
Avg.	**1.7214**	**1.9617**	**1.7283**	**4.1558**	**2.1602**	**2.0886**	**1.7400**	**1.8755**	**1.6137**	**1.7087**	**1.8374**	**1.5930**	**1.3952**

in the realization of the proposed algorithm. Fig. 5 shows the performance at different settings. It shows that $T = 2$ and an extended region of size 9×9 can provide a performance close to the optimal. Hereafter, all simulation results of the proposed algorithm presented in this paper were obtained with this setting.

For comparison, ten existing demosaicing algorithms, including BI [7], AP [3], DUOR [4], [27], DSA [5], ACPI [10], ECI [12], PCSD [13], EECI [14], AHDDA [15], and DAFD [16], were implemented for comparison. In the realization of DUOR, the correction step described in [27] was applied to the demosaicing result of [4]. Table I tabulates the CPSNR performance of different demosaicing algorithms. The proposed algorithm produces the best average performance among the tested algorithms. It was found that the proposed algorithm could handle fine texture patterns well. For images which contain many fine texture patterns such as images 6, 8, 16, and 19, the proposed method obviously outperforms the other demosaicing solutions. For example, as far as image 8 is concerned, the CPSNR achieved by the proposed algorithm is 1.21 dB higher than that of the CPSNR achieved by EECI, which is the second best among all evaluated algorithms in a way that it achieved the second best average CPSNR performance in the simulation.

Figs. 6–8 show some demosaicing results of images 1, 15, and 19 for comparison. They show that the proposed algorithm can preserve fine texture patterns and, accordingly, produce less color artifacts. Recall that the proposed algorithm is actually developed based on ACPI. As compared with ACPI, the proposed algorithm produces a demosaicing result of much less color artifact by interpolating missing components along a better direction. In fact, the average CPSNR of the proposed algorithm (39.93 dB) is much closer than that of ACPI (36.88 dB) to that achieved by the ideal ACPI (41.02 dB). These results show that the gradient test proposed in the proposed algorithm is more reliable than that of ACPI.

Table II shows the performance of various algorithms in terms of CIELab color difference [26]. The proposed algorithm provided the best performance among the evaluated algorithms again. With the proposed gradient testing tool, a simple heuristic algorithm can provide a subjectively and objectively better demosaicing performance as compared with many advanced algorithms [3]–[5], [10], [12]–[15].

The proposed algorithm is developed based on the fact that the interpolation direction for each missing green sample is critical to the final demosaicing result. A study was carried out to investigate how significant the improvement with respect to

TABLE III
MSE CONTRIBUTED BY DIFFERENT GROUPS OF PIXELS

	Group 1		Group 2		Group 3	
Pixel nature of the group	$D_{ACPI} = D_{iACPI} \neq D_{ours}$		$D_{ACPI} \neq D_{iACPI} = D_{ours}$		$D_{ACPI} \neq D_{iACPI} \neq D_{ours}$	
	ACPI	Ours w/o refinement	ACPI	Ours w/o refinement	ACPI	Ours w/o refinement
% of pixels	17.12%		19.07%		34.84%	
MSE/pixel	8.537	28.779	64.341	7.231	31.766	22.670

TABLE IV
ARITHMETIC OPERATIONS REQUIRED BY THE PROPOSED ALGORITHM TO ESTIMATE TWO MISSING COLOR COMPONENTS AT (a) A RED/BLUE SAMPLING POSITION OR (b) A GREEN SAMPLING POSITION

	Original version				Simplified version			
	ADD	**MUL**	**SHT**	**CMP**	**ADD**	**MUL**	**SHT**	**CMP**
Edge/non-edge block classification	24	1	0	2	24	1	0	2
Estimating missing green sample								
Case: edge block	9	0	5	0	9	0	5	0
Case: In non-edge block	95	39	11	2	59	4	7	2
Estimating missing red/blue sample	4	0	1	0	4	0	1	0
Refinement	19	14	0	0	19	14	0	0
Total								
Case: edge block	**56**	**15**	**6**	**2**	**56**	**15**	**6**	**2**
Case: non-edge block	**142**	**54**	**12**	**4**	**106**	**19**	**8**	**4**

(a)

	Original version				Simplified version			
	ADD	**MUL**	**SHT**	**CMP**	**ADD**	**MUL**	**SHT**	**CMP**
Estimating missing red sample	2	0	1	0	2	0	1	0
Estimating missing blue sample	2	0	1	0	2	0	1	0
Refinement	34	18	0	0	34	18	0	0
Total	**38**	**18**	**2**	**0**	**38**	**18**	**2**	**0**

(b)

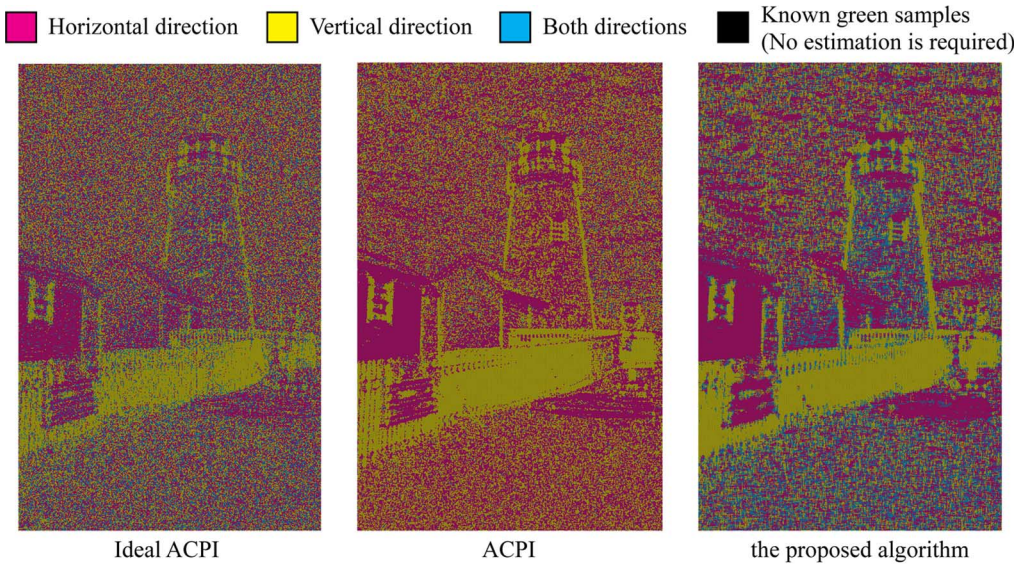

Fig. 9. Direction maps obtained with different algorithms for interpolating missing green samples.

ACPI could be when the proposed algorithm was used to find a better interpolation direction for a pixel. Note that demosaicing along edges in a natural image significantly reduces the demosaicing error. Fig. 9 shows some interpolation direction maps obtained with ACPI, the ideal ACPI and the proposed algorithm for comparison.

Table III shows the performance of ACPI and the proposed algorithm in finding an appropriate interpolation direction. This Table shows the contribution of three different groups of pixels to the MSE of the green plane in the final demosaicing result. Pixels in the testing images are grouped according to the following three constraints: (1) $D_{\mathrm{ACPI}} = D_{i\mathrm{ACPI}} \neq D_{\mathrm{ours}}$, (2) $D_{\mathrm{ACPI}} \neq D_{i\mathrm{ACPI}} = D_{\mathrm{ours}}$, and (3) $D_{\mathrm{ACPI}} \neq D_{i\mathrm{ACPI}} \neq D_{\mathrm{ours}}$, where $D_{\mathrm{ACPI}}, D_{i\mathrm{ACPI}}$, and D_{ours} are, respectively, a pixel's interpolation directions estimated with ACPI, the ideal ACPI and the proposed algorithm. One can see that the percentage of Group 2 pixels is higher than that of Group 1 pixels. This implies that, when the proposed algorithm is used, there are more hits on $D_{i\mathrm{ACPI}}$. Even in the case of $D_{i\mathrm{ACPI}} \neq D_{\mathrm{ours}}$, the estimate of the proposed algorithm is better in a way that the interpolation result provides a lower MSE. One can see the reduction in MSE/pixel achieved by the proposed algorithm in Group 3 pixels. Besides, the average penalty introduced by Group 1 pixels to the proposed algorithm is just $20.3 (= 28.8 - 8.5)$ while the average penalty introduced by Group 2 pixels to ACPI is $57.1 (= 64.3 - 7.2)$ in terms of MSE per pixel.

To a certain extent, the proposed algorithm is robust to the estimation result of ${}_H\sigma^2_{i,j}$,${}_V\sigma^2_{i,j}$, and ${}_B\sigma^2_{i,j}$. In one of our simulations, for each (i,j), ${}_H\sigma^2_{i,j}$,${}_V\sigma^2_{i,j}$, and ${}_B\sigma^2_{i,j}$ were separately corrupted by adding a uniformly distributed random noise of range $\pm 10\%$ of their original estimated values to them. It was found that the final demosaicing results were more or less the same as the one without corruption in terms of both CIELab color difference and CPSNR.

Table IV shows the complexity of the proposed algorithm. Note that some intermediate computation results can be reused during demosaicing and this was taken into account when the complexity of the proposed algorithm was estimated. Its complexity can be reduced by simplifying the estimation of ${}_H\sigma^2_{i,j}$,${}_V\sigma^2_{i,j}$ and ${}_B\sigma^2_{i,j}$. In particular, (11), (12), and (17) can be simplified by replacing Ψ with $\Psi_s = \{0, \pm 2, \pm 4\}$ and turning all involved square operations into absolute value operations. Some demosaicing performance is sacrificed due to the simplification. The simplified version provided an average CPSNR of 39.89 dB and an average CIELAB color difference of 1.6007 in our simulations. Its complexity is also shown in Table IV. In our simulations, the average execution times for the proposed algorithm and its simplified version to process an image on a 2.8-GHz Pentium 4 PC with 512-MB RAM are, respectively, 0.2091 and 0.1945 s.

V. Conclusion

In this paper, an adaptive demosaicing algorithm was presented. It makes use of the color difference variance of the pixels located along the horizontal axis and that along the vertical axis in a local region to estimate the interpolation direction for interpolating the missing green samples. With such an arrangement, the interpolation direction can be estimated more accurately, and, hence, more fine texture pattern details can be preserved in the output. Simulation results show that the proposed algorithm is able to produce a subjectively and objectively better demosaicing results as compared with a number of advanced algorithms.

Acknowledgment

The authors would like to thank Dr. B. K. Gunturk at Lousisiana State University and Dr. X. Li at University of West Virginia for providing programs of their demosaicking algorithms [3], [5].

References

[1] B. E. Bayer, "Color Imaging Array," U.S. Patent 3 971 065, Jul. 1976.
[2] B. K. Gunturk, J. Glotzbach, Y. Altunbask, R. W. Schafer, and R. M. Mersereau, "Demosaicing: Color filter array interpolation," *IEEE Signal Process. Mag.*, vol. 22, no. 1, pp. 44–54, Jan. 2005.
[3] B. K. Gunturk, Y. Altunbasak, and R. M. Mersereau, "Color plane interpolation using alternating projections," *IEEE Trans. Image Process.*, vol. 11, no. 9, pp. 997–1013, Sep. 2002.
[4] D. D. Muresan and T. W. Parks, "Demosaicing using optimal recovery," *IEEE Trans. Image Process.*, vol. 14, no. 2, pp. 267–278, Feb. 2005.
[5] X. Li, "Demosaicing by successive approximation," *IEEE Trans. Image Process.*, vol. 14, no. 3, pp. 370–379, Mar. 2005.
[6] D. Alleyson, S. Susstrunk, and J. Herault, "Linear demosaicing inspired by human visual system," *IEEE Trans. Image Process.*, vol. 14, no. 4, pp. 439–449, Apr. 2005.
[7] T. Sakamoto, C. Nakanishi, and T. Hase, "Software pixel interpolation for digital still camera suitable for a 32-bit MCU," *IEEE Trans. Consum. Electron.*, vol. 44, no. 4, pp. 1342–1352, Nov. 1998.
[8] D. R. Cok, "Signal Processing Method and Apparatus for Producing Interpolated Chrominance Values in a Sampled Color Image Signal," U.S. Patent 4 642 678, 1987.
[9] W. T. Freeman, "Median Filter for Reconstructing Missing Color Samples," U.S. Patent 4 724 395, 1988.
[10] J. F. Hamilton and J. E. Adams, "Adaptive Color Plane Interpolation in Single Sensor Color Electronic Camera," U.S. Patent 5 629 734, 1997.
[11] R. Lukac and K. N. Plataniotis, "Normalized color-ratio modeling for CFA interpolation," *IEEE Trans. Consum. Electron.*, vol. 50, no. 2, pp. 737–745, May 2004.
[12] S. C. Pei and I. K. Tam, "Effective color interpolation in CCD color filter arrays using signal correlation," *IEEE Trans. Circuits Syst. Video Technol.*, vol. 13, no. 6, pp. 503–513, Jun. 2003.
[13] X. Wu and N. Zhang, "Primary-consistent soft-decision color demosaicing for digital cameras," *IEEE Trans. Image Process.*, vol. 13, no. 9, pp. 1263–1274, Sep. 2004.
[14] L. Chang and Y. P. Tam, "Effective use of spatial and spectral correlations for color filter array demosaicing," *IEEE Trans. Consum. Electron.*, vol. 50, no. 1, pp. 355–365, Feb. 2004.
[15] K. Hirakawa and T. W. Parks, "Adaptive homogeneity-directed demosaicing algorithm," *IEEE Trans. Image Process.*, vol. 14, no. 3, pp. 360–369, Mar. 2005.
[16] R. Lukac and K. N. Plataniotis, "Data-adaptive filters for demosaicking: A framework," *IEEE Trans. Consum. Electron.*, vol. 51, no. 2, pp. 560–570, May 2005.
[17] R. Lukac and K. N. Plataniotis, "Fast video demosaicking solution for mobile phone imaging applications," *IEEE Trans. Consum. Electron.*, vol. 51, no. 2, pp. 675–681, May 2005.
[18] A. Lukin and D. Kubasov, "An improved demosaicing algorithm," presented at the Graphicon, Moscow, Russia, Sep. 2004.
[19] R. Ramanath and W. E. Snyder, "Adaptive demosaicking," *J. Electron. Imag.*, vol. 12, no. 4, pp. 633–642, Oct. 2003.
[20] W. Lu and Y. P. Tang, "Color filter array demosaicking: New method and performance measures," *IEEE Trans. Image Process.*, vol. 12, no. 10, pp. 1194–1210, Oct. 2003.
[21] R. Lukac, K. N. Plataniotis, D. Hatzinakos, and M. Aleksic, "A novel cost effective demosaicking approach," *IEEE Trans. Consum. Electron.*, vol. 50, no. 1, pp. 256–261, Feb. 2004.
[22] N. Kehtarnavaz, H. J. Oh, and Y. Yoo, "Color filter array interpolation using color correlations and directional derivatives," *Electron. Imag. J.*, vol. 12, no. 4, pp. 621–632, Oct. 2003.
[23] J. Adams, "Design of practical color filter array interpolation algorithms for digital cameras," *Proc. SPIE* , vol. 3028, pp. 117–125, Feb. 1997.
[24] R. Lukac, K. Martin, and K. N. Plataniotis, "Demosaicked image postprocessing using local color ratios," *IEEE Trans. Circuits Syst. Video Technol.*, vol. 14, no. 6, pp. 914–920, Jun. 2004.
[25] R. Lukac and K. N. Plataniotis, "A robust, cost-effective postprocessor for enhancing demosaicked camera images," *Real-Time Imag.*, vol. 11, no. 2, pp. 139–150, Apr. 2005.

[26] K. McLaren, "The development of the CIE 1976 (L*a*b*) uniform color-space and colour-difference formula," *J. Soc. Dyers and Colourists*, pp. 338–341, 1976.
[27] D. D. Muresan and T. W. Parks, "Optimal recovery demosaicing," presented at the IASTED Signal and Image Processing, Hawaii, 2002.

King-Hong Chung received the B.Eng. (Hons.) degree in electronic and information engineering form the Hong Kong Polytechnic University in 2001, where he is currently pursing the M.Phil. degree.

His research interests include digital image halftoning, image compression, and digital camera image processing.

Yuk-Hee Chan (M'92) received the B.Sc. degree (Hons.) in electronics from Chinese University of Hong Kong in 1987 and the Ph.D. degree in signal processing from Hong Kong Polytechnic University in 1992.

Between 1987 and 1989, he was an R & D Engineer at Elec & Eltek Group, Hong Kong. He joined The Hong Kong Polytechnic University in 1992 and is now an Associate Professor with the Department of Electronic and Information Engineering. He has published over 100 research papers in various international journals and conferences. His research interests include image and video compression, image restoration, and fast computational algorithms in DSP.

Dr. Chan is a member of Institution of Electrical Engineers.